Lasing of ambient air with microjoule pulse energy pumped by a multi terawatt IR femtosecond laser

Guillaume Point, Yi Liu, Yohann Brelet, Sergey Mitryukovskiy, Pengji Ding, Aurélien Houard, André Mysyrowicz

▶ **To cite this version:**

Guillaume Point, Yi Liu, Yohann Brelet, Sergey Mitryukovskiy, Pengji Ding, et al.. Lasing of ambient air with microjoule pulse energy pumped by a multi terawatt IR femtosecond laser. Optics Letters, 2014, 39, pp.1725. 10.1364/OL.39.001725 . hal-01118170

HAL Id: hal-01118170

https://ensta-paris.hal.science/hal-01118170

Submitted on 18 Feb 2015

HAL is a multi-disciplinary open access archive for the deposit and dissemination of scientific research documents, whether they are published or not. The documents may come from teaching and research institutions in France or abroad, or from public or private research centers.

L'archive ouverte pluridisciplinaire **HAL**, est destinée au dépôt et à la diffusion de documents scientifiques de niveau recherche, publiés ou non, émanant des établissements d'enseignement et de recherche français ou étrangers, des laboratoires publics ou privés.

Lasing of ambient air with microjoule pulse energy pumped by a multi terawatt IR femtosecond laser

Guillaume Point, Yi Liu*, Yohann Brelet, Sergey Mitryukovskiy, Pengji Ding, Aurélien Houard, and André Mysyrowicz[+]
[1] *Laboratoire d'Optique Appliquée, ENSTA ParisTech/CNRS/Ecole Polytechnique, 828, Boulevard des Maréchaux, Palaiseau, 91762, France*
**Corresponding author: yi.liu@ensta-paristech.fr; [+]andre.mysyrowicz@ensta-paristech.fr*

We report on the lasing action of atmospheric air pumped by an 800 nm femtosecond laser pulse with peak power up to 4 TW. Lasing emission at 428 nm increases rapidly over a small range of pump laser power, followed by saturation above ~ 1.5 TW. The maximum lasing pulse energy is measured to be 2.6 μJ corresponding to an emission power in the MW range, while a maximum conversion efficiency of 3.5×10^{-5} is measured at moderate pump pulse energy. The optical gain inside the filament plasma is estimated to be excess of 0.7/cm. The lasing emission shows a doughnut profile, reflecting the spatial distribution of the pump-generated white-light continuum that acts as a seed for the lasing. We attribute the pronounced saturation to the defocusing of the seed in the plasma amplifying region and to the saturation of the seed intensity.
OCIS Codes: (320.7120) Ultrafast phenomena (140.4130) Molecular gas lasers

Stimulated emission from air plasma columns has attracted wide attention because of its potential application for remote sensing [1-12]. Backward Amplified Spontaneous Emissions (ASE) originated from both nitrogen and oxygen molecules have been obtained under different laser excitation conditions [1-3]. In 2011, J. Yao and co-workers reported several strong stimulated emission lines in the forward direction in ambient air or pure nitrogen [7]. These radiation lines at 391, 428, and 471 nm can be activated either by a wavelength tunable mid-infrared laser (1.29 μm - 4 μm) or an 800 nm femtosecond pulse together with an additional seed pulse at a proper wavelength [7-9]. Forward single pass lasing of these emission lines has been attributed to the following mechanism: rapid population inversion between the $B^2\Sigma_u^+$ and $X^2\Sigma_g^+$ states of the N_2^+ induced by the pump laser, followed by seeded amplification. The seed is either the 3rd and/or 5th harmonic signal of the mid-infrared pump or an external seed pulse around 400 nm in the case of the 800 nm pump.

Very recently, three groups have independently reported self-seeded forward lasing action from N_2^+ in air or pure nitrogen pumped by just one single pulse at 800 nm [10-12]. Seeding in this case is provided by the generation of 2nd harmonic and supercontinuum white-light inside the gas [10-12]. Discovery of the self-seeded air lasing effect pumped by the widely available 800 nm femtosecond laser simplifies the experimental setup and offers the possibility of scaling up to Terawatt (TW) class pump lasers. In previous experiments so far, however, the IR pump power was limited to a few tens of GW [7-12]. Consequently, the energy of the lasing emission was too weak to be measured.

In this letter, we study self-seeded lasing from laser filaments in ambient air driven by 800 nm femtosecond pulses with a peak power of 4 TW. In the experiment, we used the Enstamobile laser system which delivers 50 fs laser pulses at a repetition rate of 10 Hz with pulse energy up to 300 mJ. The beam exhibits a super-Gaussian profile with a diameter of 40 mm (FMHM). The output pulses were focused by a convex lens of focal length f = 100, 150 and 200 cm. Best results were obtained with the f = 100 cm lens. After the plasma, two pieces of glass filters (BG 40) were installed in the beam to remove the strong infrared driving pulse and the accompanying white light with wavelength longer than 650 nm. For detection, a convex lens of f = 10 cm was used to collect the radiation into a fibre spectrometer (HR 4000, Ocean Optics). The energy of the lasing emission was measured with a sensitive laser pulse energy meter (model: OPHIR, NOVA, PE9-C). We also measured the spatial profile of the lasing radiation with a charge-coupled device (CCD) camera.

In Fig. 1, we present the measured spectrum of the forward UV radiation as a function of incident laser pulse energy. At ambient pressure, the only line showing significant gain is at 428 nm. It appears as a narrow-band emission peak superimposed upon the tail of a broad continuum extending to larger wavelength for pump pulse powers larger than 150 GW (7.5 mJ). Upon increase of the incident laser power, the radiation at 428 nm increases progressively and shows saturation beyond P = 1.5 TW, as shown in Fig. 2. The measured width (FWHM) of this radiation was 1.2 nm, limited by the resolution of the spectrometer. Note that the real spectral width is on the order of ~ 0.1 nm [13]. This radiation line has been identified as due to the transition between the second excited state ($B^2\Sigma_u^+(v=0)$) of the N_2^+ and its ground state ($X^2\Sigma_g^+(v'=1)$), where v and v' denote the molecular vibrational quantum number of the corresponding states [10-12]. In all our experiment, lasing radiation at 391 nm was rarely observed and was very weak compared to that around 428 nm.

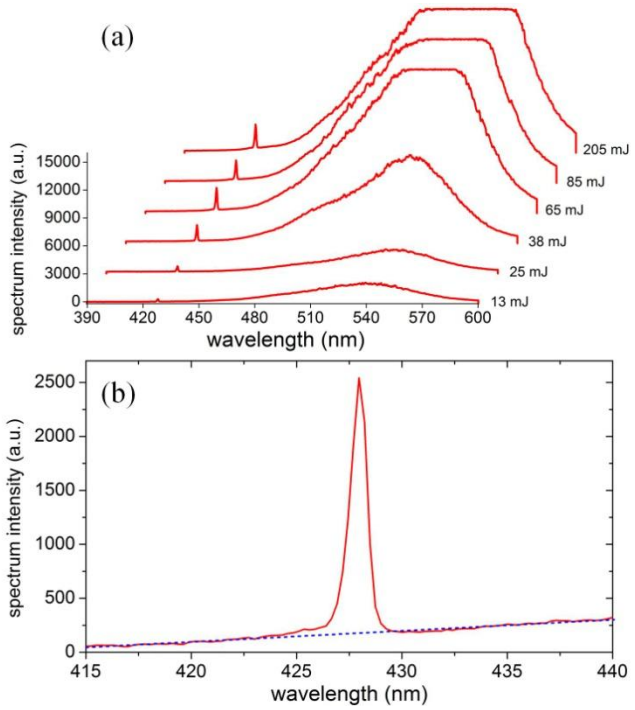

Fig. 1. (a), Spectrum of the forward emission after filamentation of laser pulses in ambient air. The focal length was 100 cm. (b), Zoomed spectrum around 428nm in the case of E_{in} = 65 mJ. The dotted line shows the estimated contribution of the supercontinuum white-light.

We estimated the optical gain inside the filaments plasma as $g = \ln[I_{out}/I_{seed}]/L$, where I_{out}, I_{seed}, and L are the output lasing intensity, the seed lasing intensity and the effective length of the plasma amplifier. In Fig. 1(b), we present the zoomed forward spectrum in the case of E_{in} = 65 mJ. The optical gain is therefore determined to be $g = \ln[2546/172]/3.95 = 0.7/cm$. This gain value is probably seriously underestimated here due to the limited spectral resolution of the spectrometer, which results in an order of magnitude decrease of the observed peak emission intensity at 428 nm. The gain per unit length for a high pressure gas laser reads

$$g = \frac{(c^2/8\pi\nu^2)(N'-N)}{\Delta\nu\tau} \qquad (1)$$

where $(N'-N)$ is the population inversion per unit length, ν and $\Delta\nu = Z/\pi$ are the frequency of the laser emission and the line width with Z the molecule collision frequency, τ is the radiative lifetime [14]. Taking $Z = 6.52\times10^9/s$ at standard temperature and pressure and $\tau \approx 100$ ns [15], we calculated $(N'-N)$ to be 1.8 × 10^{16}/cm. The population inversion density per volume can then be estimated to be 4 × 10^{17}/cm^3, by considering a transverse plasma size of ~ 1.2 mm which will be discussed below.

We measured the energy of the lasing radiation at 428nm with the laser energy meter equipped with an interference filter at 428 nm (10 nm bandwidth). The net energy of the lasing radiation was calibrated with careful consideration of the spectrum weight of the lasing emission in the total transmitted radiation, the reflection loss of the exit fused silica windows and the collecting lens, the transmission property of the BG 40 color filter and of the interference filter. A calibrated energy of 2.6 μJ was deduced for the 428 nm lasing emission with P_{in} = 2.4 TW. The maximum conversion efficiency was found to be 3.5×10^{-5} for a pump pulse power of 1.3 TW.

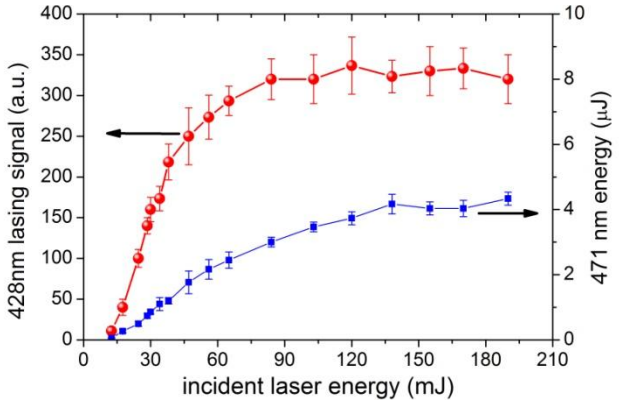

Fig. 2. Dependence of the 428 nm lasing signal and the 471nm white-light spectrum component energy as a function of the incident laser pulse energy.

We measured the spatial profile of the 428 nm lasing radiation with a CCD camera equipped with the same interference filter. The results are presented in Fig. 3(a)-3(d). The radiation shows a doughnut-shaped pattern, with a slight increase of its opening angle for higher incident pulse energies. In Fig. 3(a), the divergence angle of the emission was estimated to be 18.6 mrad. Such a small angle confirmed again the stimulated radiation nature of this emission. In a previous work, we tentatively attributed this doughnut-shaped radiation to the conical shape of the seeding white-light pulses [10]. Here we examine this hypothesis in more details. First, we monitored the spatial distribution of the broadband continuum at a wavelength close to the seed at 428 nm. The profile of the white-light component around 471 nm (10 nm bandwidth), shown in Fig. 3(e), displays a similar doughnut shape. Next, we checked the profile of the entire white-light emission on a screen installed 3 meters away from the geometric focus of the f = 1 m focusing lens. The result presented in Fig. 3(f), shows a darker central area surrounded by visible radiation with different colors. Based on the above two observations, we conclude that the spatial distribution of the white-light seeding pulse is at the origin of the doughnut shaped 428 nm single pass lasing. Such conical emission has been widely observed during filamentation in air and solid and several mechanisms have been proposed for its explanation [16].

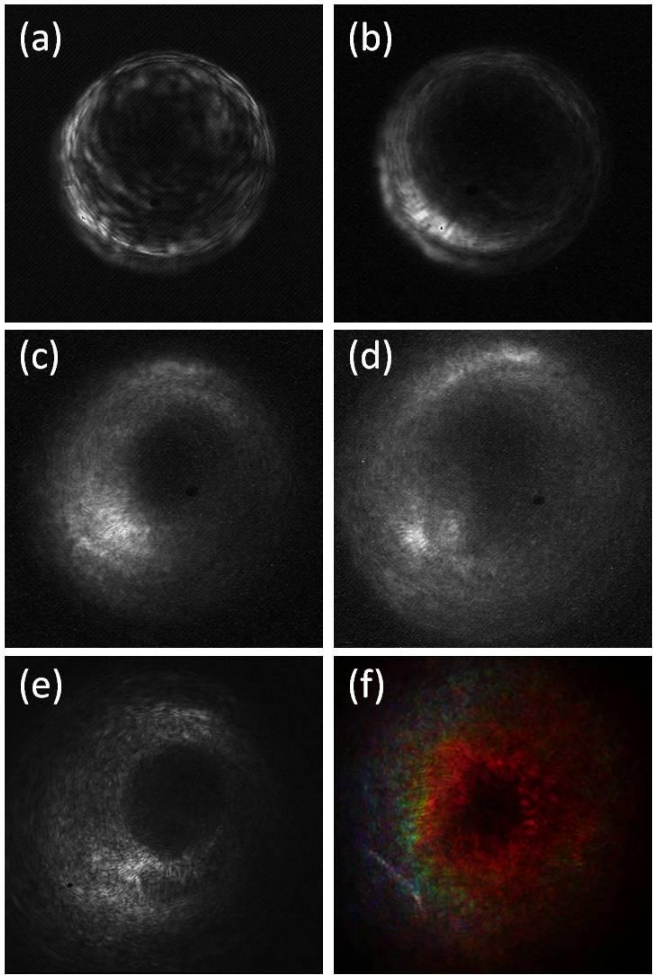

Fig. 3. (a)-(d), Spatial profiles of the 428 nm lasing radiation for different incident laser energies. The incident laser pulse energy was 18, 30, 103, and 205 mJ, respectively. (e), Profile of the white-light component around 471 nm. (f), Image of the total white-light conical emission on a screen situated 3 m away from the focal length. For (e) and (f), the incident laser energy was 80 mJ.

Delete Four key factors for the single pass lasing from filaments can be identified, namely the incident seed pulse energy, the density of population inversion, the volume of the plasma amplifier, and the spatial overlap between the seeding pulse and the amplifying plasma media. The role of the first three factors are expected to be similar to that in a traditional laser amplifier [17], while the last factor is particular for this filaments amplifier due to the non uniform transverse profile of the laser intensity , the plasma nature of the amplifier, and the formation of multiple filaments [18]. In the following, we examine the evolution of these factors as a function of the incident IR pulse energy.

We first checked the volume of the filaments plasma amplifier. The images of the filaments taken by a CCD camera are presented in Fig. 4 as a function of incident laser pulse energy. The length and width of the filaments are seen to increase at higher pulse energy. When the pulse energy exceeds 84 mJ, clear evidence for multiple filaments formation at the initial stage of filamentation is observed (Fig. 4 (e)-4(g)). We numerically integrated each rows (lines) of the fluorescence plasma track and defined the plasma channel length (width) by $1/e^2$ of the maximum value. The results are presented in Fig. 5 (a). The plasma volume is estimated as $V = \pi(d/2)^2 \times L$, where d and L are the length and width of the plasma respectively. We show the results in Fig. 5(b), where a monotonous increase is observed at higher pump pulse energies.

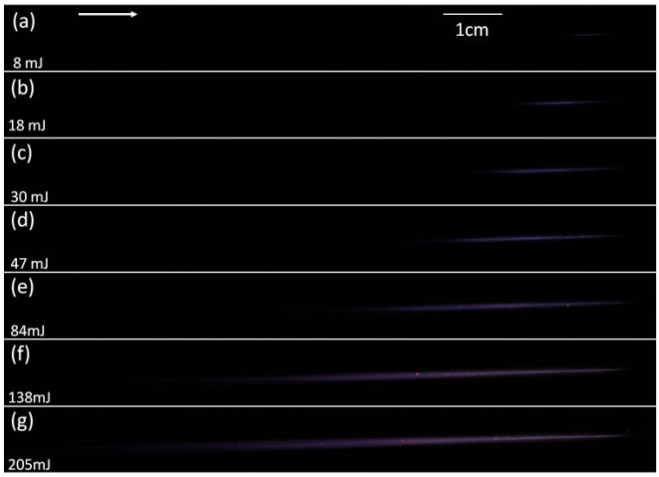

Fig. 4. Images of the filaments with different incident pulse energies, as indicated in each panel. The arrow in (a) denotes the direction of laser propagation.

We next discuss the density of population inversion. The mechanism for population inversion is still a matter of controversy [7-12]. As a result, a direct evaluation of population inversion inside the plasma channel is impossible at this stage. Nevertheless, it is reasonable to assume that the population inversion is related to the pump laser intensity, based on the observation that the population inversion is achieved within the driven pulse duration [8, 9]. It is known that the laser intensity inside a single filament remains almost unchanged, or "clamped" for a given focusing geometry above a critical power threshold, due to the interplay between the Kerr self-focusing effect and the plasma defocusing effect [19]. In the case of many filaments compressed to a bundle, the peak intensity can increase above the clamping value, as we will report elsewhere. Therefore, we expect that the density of population inversion is either roughly constant or even increases in our experiment. Since the amplifying medium increases while its population inversion density increases or stays constant, the saturation must have another origin.

We now discuss the dependence of the seed pulse energy with pump energy. Lasing action occurs at the spectrum position of the seed pulse, which prohibits a net measurement of the seed pulse energy as a function of pump laser energy in the absence of gain. Therefore, we analyzed the evolution of the seed pulse energy at another closely spaced wavelength, at 471 nm with a bandwidth of 10 nm.

The results are presented in Fig. 2. Upon increase of the pump pulse energy, the white light spectrum around 471 nm increases and progressively saturates, but the saturation is less pronounced than for the lasing signal. Therefore, the strong saturation of the 428 nm lasing radiation for P_{in} > 1.5 TW is not due solely to the saturation of the seeding pulse.

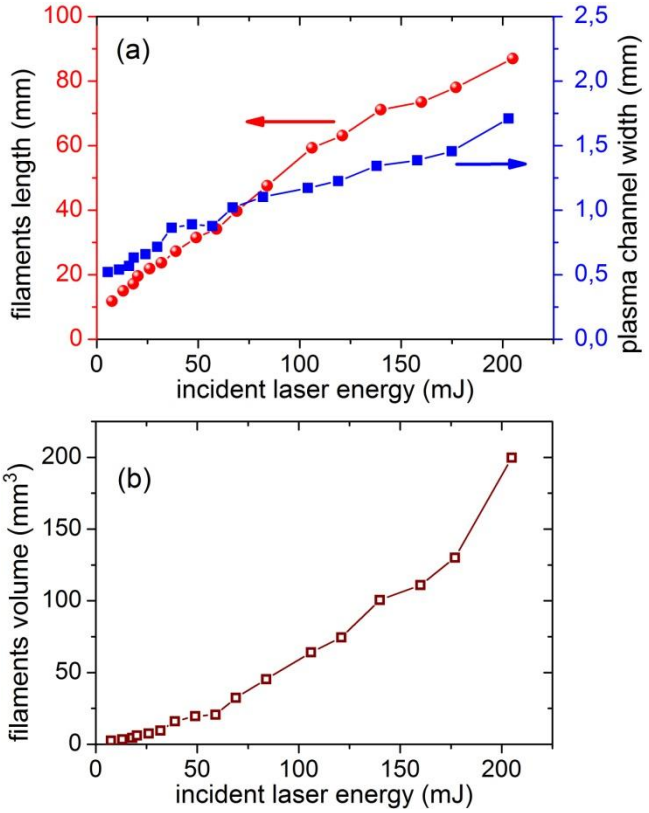

Fig. 5. (a), Length and width of the plasma channel as a function of the incident laser energy. (b), Calculated filaments volume.

Finally, we discuss the degree of spatial overlap between the seeding pulse and active amplifying region. Since the amplifying region is a plasma, it acts as a defocusing medium. Under the joint action of self-focusing and plasma defocusing, the fundamental laser pulse and the accompanying white-light supercontinuum can form complex transverse distribution inside the filaments [18], which deteriorates the spatial overlap between the seeding pulse and amplifying plasma. As presented in Fig. 3(e) and 3(f), the non uniform character of the seeding pulse transverse profile is apparent in the far field distribution. In addition, the formation of multiple filaments can exacerbate the transverse non-uniformity of the plasma amplifier. We therefore speculate that the plasma defocusing effect also plays an important role for the saturation of the lasing yield when P_{in} becomes larger than 1.5 TW.

To conclude, the above experimental observations show that upon increase of pump pulse energy, the density of population inversion keeps unchanged or increases, while the plasma amplifier volume increases considerably. Consequently, the gain saturation cannot be explained by complete depletion of the population inversion. To the contrary, our analysis indicates that there is room for an increase in lasing efficiency in air with TW lasers. On the other hand, the white-light seed pulse shows pronounced saturation and most probably experiences defocusing during its propagation in the amplifying plasma medium. We believe that these last two factors are at the origin of the lasing yield saturation.

In summary, we observed lasing action of atmospheric air pumped by 800 nm laser pulses with peak power up to 4 TW. The radiation yield first increases rapidly but saturates for pulse power larger than 1.5 TW. The maximum lasing radiation energy was 2.6 μJ and the maximum conversion efficiency was 3.5×10^{-5}. We attribute the lasing energy saturation to the sub-linear increase of the seed pulse with increasing pump power and the effect of plasma defocusing on the seed propagation.

References:

[1]Q. Luo, W. Liu, and S. L. Chin, Appl. Phys. B **76**, 337 (2003).

[2]D. Kartashov, S. Ališauskas, G. Andriukaitis, A. Pugžlys, M. Shneider, A. Zheltikov, S. L. Chin, and A. Baltuška, Phys. Rev. A **86**, 033831 (2012).

[3]A. Dogariu, J. B. Michael, M. O. Scully, and R. B. Miles, Science **331**, 442 (2011).

[4]P. Sprangle, J. Peñano, B. Hafizi, D. Gordon, and M. Scully, Appl. Phys. Lett. **98**, 211102 (2011).

[5]M. N. Shneider, A. Baltuška, and A. M. Zheltikov, J. Appl. Phys. **110**, 083112 (2011).

[6]P. R. Hemmer, R. B. Miles, P. Polynkin, T. Siebert, A. V. Sokolov, P. Sprangle, and M. O. Scully, *Proc. Natl. Acad. Sci. USA* **108,** 3130 (2011).

[7]J. Yao, B. Zeng, H. Xu, G. Li, W. Chu, J. Ni, H. Zhang, S. L. Chin, Y. Cheng, and Z. Xu, Phys. Rev. A **84**, 051802(R) (2011).

[8]J. Ni, W. Chu, C. Jing, H. Zhang, B. Zeng, J. Yao, G. Li, H. Xie, C. Zhang, H. Xu, S. L. Chin, Y. Cheng, and Z. Xu, Opt. Express, **21**, 8746 (2013).

[9]J. Yao, G. Li, C. Jing, B. Zeng, W. Chu, J. Ni, H. Zhang, H. Xie, C. Zhang, H. Li, H. Xu, S. L. Chin, Y. Cheng, and Z. Xu, New J. Phys. **15**, 023046 (2013).

[10]Y. Liu, Y. Brelet, G. Point, A. Houard, and A. Mysyrowicz, Opt. Express, **21**, 22791 (2013).

[11]T. Wang, J. Ju, J. F. Daigle, S. Yuan, R. Li, and S. L. Chin, Las. Phys. Lett. **10**, 125401 (2013).

[12]W. Chu, G. Li, H. Xie, J. Ni, J. Yao, B. Zeng, H. Zhang, C. Jing, H. Xu, Y. Cheng, and Z. Xu, Las. Phys. Lett. **10**, 125401 (2013).

[13] F. Emmert, R. Dux, and H. Langhoff, Appl. Phys. B **47**, 141(1988).

[14] J. D. Anderson, Gasdynqmic lasers: an introduction, Academic Press, 1976.

[15] A. Lofthus and P. H. Krupenie, J. Phys. Chem. Ref. Data. **6**, 113 (1977).

[16] A. Couairon and A. Mysyrowicz, Phys. Rep. 441, 47 (2007).

[17] *A. E. Siegman*, *Lasers*, University Science Books, Mill Valley, CA (1986).

[18] S. L. Chin, N. Aközbek, A. Proulx, S. Petit, and C. M. Bowden, Opt. Commun. **188**, 181 (2001).

[19] A. Becker, N. Aközbek, K. Vijayalakshmi, E. Oral, C. M. Bowden, S. L. Chin, Appl. Phys. B **73**, 287 (2001).

References with titles:

[1]Q. Luo, W. Liu, and S. L. Chin, "Lasing action in air induced by ultra-fast laser filamentation," Appl. Phys. B **76**, 337 (2003).

[2]D. Kartashov, S. Ališauskas, G. Andriukaitis, A. Pugžlys, M. Shneider, A. Zheltikov, S. L. Chin, and A. Baltuška, "Free-space nitrogen gas laser driven by a femtosecond filament," Phys. Rev. A **86**, 033831 (2012).

[3]A. Dogariu, J. B. Michael, M. O. Scully, and R. B. Miles, "High-gain backward lasing in air," Science **331**, 442 (2011).

[4]P. Sprangle, J. Peñano, B. Hafizi, D. Gordon, and M. Scully, "Remoely induced atmospheric lasing," Appl. Phys. Lett. **98**, 211102 (2011).

[5]M. N. Shneider, A. Baltuška, and A. M. Zheltikov, "Population inversion of molecular nitrogen in an Ar: N2 mixture by selective resonance-enhanced multiphon ionizatoin," J. Appl. Phys. **110**, 083112 (2011).

[6]P. R. Hemmer, R. B. Miles, P. Polynkin, T. Siebert, A. V. Sokolov, P. Sprangle, and M. O. Scully, "Standoff spectroscopy via remote generation of a backward-propagating laser beam,"*Proc. Natl. Acad. Sci. USA* **108,** 3130 (2011).

[7]J. Yao, B. Zeng, H. Xu, G. Li, W. Chu, J. Ni, H. Zhang, S. L. Chin, Y. Cheng, and Z. Xu, "High-brightness switchable multiwavelength remote laser in air," Phys. Rev. A **84**, 051802(R) (2011).

[8]J. Ni, W. Chu, C. Jing, H. Zhang, B. Zeng, J. Yao, G. Li, H. Xie, C. Zhang, H. Xu, S. L. Chin, Y. Cheng, and Z. Xu, "Identification of the physical mechanism of generation of coherent N_2^+ emission in air by femtosecond laser excitation," Opt. Express, 2**1**, 8746 (2013).

[9]J. Yao, G. Li, C. Jing, B. Zeng, W. Chu, J. Ni, H. Zhang, H. Xie, C. Zhang, H. Li, H. Xu, S. L. Chin, Y. Cheng, and Z. Xu, "Remote creation of coherent emissions in air with two-color ultrafast laser pulses," New J. Phys. **15**, 023046 (2013).

[10]Y. Liu, Y. Brelet, G. Point, A. Houard, and A. Mysyrowicz, "Self-seeed lasing in ionized air pumped by 800 nm femtosecond laser pulses," Opt. Express, **21**, 22791 (2013).

[11]T. Wang, J. Ju, J. F. Daigle, S. Yuan, R. Li, and S. L. Chin, "Self-seeded forward lasing action from a femtosecond Ti:sapphire laser filament in air," Las. Phys. Lett. **10**, 125401 (2013).

[12]W. Chu, G. Li, H. Xie, J. Ni, J. Yao, B. Zeng, H. Zhang, C. Jing, H. Xu, Y. Cheng, and Z. Xu, "A Self-induced white light seeding laser in a femtosecond laser filament," Las. Phys. Lett. **10**, 125401(2013).

[13] F. Emmert, R. Dux, and H. Langhoff, "Improved lasing properties of the HeN_2^+ system at 391 nm qnd 428 nm by H2 admisture," Appl. Phys. B **47**, 141(1988).

[14] J. D. Anderson, Gas dynamic lasers: an introduction, Academic Press, 1976.

[15] A. Lofthus and P. H. Krupenie, "The spectrum of nitrogen molecule"J. Phys. Chem. Ref. Data. **6**, 113 (1977).

[16] A. Couairon and A. Mysyrowicz, "Femtosecond filamentation in transparent media," Phys. Rep. 441, 47 (2007).

[17] *A. E. Siegman*, *Lasers*, University Science Books, Mill Valley, CA (1986).

[18] S. L. Chin, N. Aközbek, A. Proulx, S. Petit, and C. M. Bowden, "Transverse ring formation of a focused femtosecond laser pulse propagating in air," Opt. Commun. **188**, 181 (2001).

[19] A. Becker, N. Aközbek, K. Vijayalakshmi, E. Oral, C. M. Bowden, "Intensity clamping and re-focusing of intense femtosecond laser pulses in nitrogen molecular gas," S. L. Chin, Appl. Phys. B **73**, 287 (2001).